In: Focus on Swarm Intelligence Research and Applications ISBN: 978-1-53612-452-1
Editors: B. Benhala, P. Pereira and A. Sallem

Chapter 2

PARAMETRIC OPTIMIZATION OF LASER BEAM MACHINING PROCESSES USING A SHUFFLED FROG LEAPING ALGORITHM

Ankan Mitra and Shankar Chakraborty*
Department of Production Engineering,
Jadavpur University, Kolkata, India

ABSTRACT

Need for generation of intricate shapes on difficult-to-machine materials, better surface finish and higher material removal rate drives towards the development of an array of non-traditional machining (NTM) processes. Laser beam machining (LBM) is one such NTM process where a laser beam is directed towards the workpiece surface for material removal. With development of different NTM processes over the years, LBM process has become the first choice for machining of metallic and non-metallic workpieces, giving rise to the requirement to optimize its input parameters to achieve the best machining performance. Variation in any of these parameters (lamp current, pulse frequency, pulse width, cutting speed, assist air pressure etc.) may result in deviation in the responses (surface finish, material removal rate, heat affected zone, conicity, kerf etc.). Since in LBM process, there is a combination of multiple parameters, change in any or all of these parameters has a remarkable effect on the responses. Thus, it becomes important to study the effects of various LBM process parameters on the responses as well as to search out the best possible combination of these parameters to attain the target results. Several mathematical tools, like Taguchi method, desirability function, grey relational analysis etc. have been proposed for parametric optimization of LBM processes. In this chapter, an almost unexplored meta-heuristic in the form of shuffled frog leaping algorithm is adopted for both single and multi-objective optimization of the responses for two LBM processes. It is a nature inspired algorithm and mimics the

* Corresponding Author address, Email: s_chakraborty00@tahoo.co.in.

leaping pattern of frogs in search of food. Its major advantage is that it doesnot accumulate towards some local optima. Local exploration of frogs ensures memetic evolution within a population, whereas, global exploration makes way for a global share of information (memes) between the populations. As the leaping behavior of frogs is mimicked in this algorithm, the number of iterations required to reach the global optimum is drastically reduced. The developed scatter plots can be utilized to investigate the variationsin LBM responses with respect to changes in different process parameters involved. The derived results show a significant improvement in the response values as compared to the earlier attempts for optimization of LBM processes employing other meta-heuristics.

Keywords: laser beam machining, shuffled frog leaping algorithm, optimization, process parameter response

1. INTRODUCTION

In this present world, emergence of new technologies along with increased human needs has given rise to the need of extremely sophisticated products with high ergonomic values, requiring more intricate and complex drawings and designs. Conventional machining processes miserably fail here to provide the best results, which drive into the development of an array of different non-traditional machining (NTM) processes capable of providing quite accurate results. There are several NTM processes, like electrochemical machining, electro-discharge machining, wire electrical discharge machining, laser beam machining (LBM), electron beam machining, ion beam machining, plasma arc machining, chemical machining, ultrasonic machining, jet machining etc., which are currently being deployed in every sphere of industry for generating complex shape features on different difficult-to-machine materials. Among these, LBM process is considered to be one of the most versatile methods of machining since it can machine a wide range of advanced engineering materials. It is widely used for cutting, welding, drilling, marking and sintering operations. It is also effectively applied for turning and milling operations.

Laser machining is a technology using a laser beam source which is a narrow beam of intense monochromatic light focused on the workpiece surface to cut the required shapes of profile on metals, non-metals, ceramics etc. It is a non-contact type of machining process where there is no physical contact between the tool and the workpiece. There is another unique feature about this machining process that it can machine any material irrespective of its hardness and melting point. In this machining process, the output of a high power laser beam is directed in a programed manner towards the material required to be cut which transfers energy from the beam to the workpiece surface. The mechanism behind material removal during LBM operation includes three stages, e.g., melting, vaporizing and degrading (chemical degradation by breaking the

bonds between atoms). The high amount of heat thus generated is absorbed by the surface resulting melting, vaporization or formation of a chemically changed state, which is thereupon removed from the machining zone by the flow of a high pressure assist gas jet.

Thus, LBM is a thermal process and its effectiveness on different work materials largely depends on their thermal properties, like thermal conductivity, thermal diffusivity etc., rather than on mechanical properties, and also to some extent on their optical properties. Generally, work materials with low thermal diffusivity and conductivity are well suited for this process because these properties help in concentrating the accumulated energy at a particular place rather than flowing through the whole work material. Since energy transfer occurs through irradiations, no mechanical forces are involved during the cutting operation, which leads to no tool wear or machine vibration. Hence, the material removal rate (MRR) gets independent of the mechanical factors, such as tool force, tool chatter etc. [1].

The laser medium may be a solid (e.g., Nd:YAG or neodymium-doped yttrium-aluminum-garmet), liquid (dye) or gas (e.g., CO_2, He, Ne) [2]. Among these different types, Nd:YAG and CO_2 lasers are most widely used for material machining applications. The CO_2 laser has wavelength of 10 μm in the infrared region. It has high average beam power, better efficiency and good beam quality. It is quite suitable for fine cutting of sheet metals at high speed [3]. On the other hand, Nd:YAG laser has low beam power, but while operating on pulsed mode, high peak powers enable it to machine even thicker work materials. Its shorter pulse duration also suits for machining of thinner materials. Due to shorter wavelength (1 μm), it can be absorbed by high reflective materials which are difficult to machine using CO_2 laser [4].

An LBM operation involves several process parameters, such as assist gas pressure, pulse width, cutting speed, pulse frequency, peak power, current etc. All these parameters partially or completely affect the LBM process performance. Some of the quality characteristics of interest in LBM process are MRR, machined geometry (kerf width, hole diameter, taper), surface quality (surface roughness (SR), surface morphology), metallurgical characteristics (recast layer, heat affected zone (HAZ), dross inclusion) and mechanical properties (hardness, strength etc.). Experimental studies by Voisey et al. [5] found variations in MRR at different power densities during laser drilling operation, having a trend of first increasing and then decreasing. Lau et al. [6] showed that compressed air could remove more material in comparison to argon inert gas during laser cutting of carbon fiber composites. The MRR during laser machining of concretes showed increasing trend with respect to both laser power and scan speed [7]. Chen [8] examined the kerf width for three different assist gases, i.e., oxygen, nitrogen and argon at high pressure, and observed that kerf width would increase with increasing laser power and decreasing cutting speed during CO_2 laser cutting of 3 mm thick mild steel sheet. Other metallurgical characteristics, such as HAZ thickness etc., also need to be minimized during LBM operation. Decreasing power and increasing feed rate generally

lead to decrease in HAZ [9]. Thus, in order to understand the effects of various LBM process parameters on the responses, modeling of the complex LBM process is often required. To help in this direction, several experimental methods, like response surface methodology (RSM) with central composite design plan and Taguchi robust design methodology have mostly been utilized by the past researchers. On the other hand, analytical methods including mathematical models, such as finite difference method, finite element method, boundary element method etc. have also been deployed to understand the material removal mechanism of LBM process.

The complexity in machining dynamics has forced the researchers to search out the optimal or near optimal machining conditions in discrete and continuous parametric spaces with multi-model, differentiable or non-differentiable objective functions (responses) employing different state-of-the-art optimization techniques. In this chapter, an almost unexplored meta-heuristic in the form of shuffled frog leaping algorithm (SFLA), which is a hybrid of two conventional optimization techniques and mimics the behavioral pattern of frogs, is proposed for parametric optimization of two LBM processes.

2. LITERATURE REVIEW

Ganguly et al. [10] integrated Taguchi method with grey relational analysis (GRA) to determine the laser micro-drilling parameters in order to minimize two micro-drilling defects, i.e., hole taper and HAZ width. Employing genetic algorithm (GA), Pandey and Dubey [11] simultaneously optimized both kerf taper and SR in laser cutting of Titanium alloy sheet. Pandey and Dubey [12] integrated a robust parameter design methodology and fuzzy logic to investigate the laser cutting operation of Duralumin sheet so as to improve the geometrical accuracy while simultaneously minimizing kerf width and kerf deviations at top and bottom sides. Teixidor et al. [13] proposed a multi-criteria decision making approach for laser milling process parameter (scanning speed, pulse intensity and pulse frequency) selection for achieving the desired surface quality and dimensional accuracy while using particle swarm optimization (PSO) technique. Mukherjee et al. [14] applied artificial bee colony (ABC) algorithm for determining the optimal Nd:YAG LBM process parameters while considering both single and multi-objective optimization of the responses. Pandey and Dubey [15] concurrently optimized multiple responses (cut edge surface roughness, kerf taper and kerf width) of a laser cutting process while employing a hybrid approach combining GRA and fuzzy logic. Chaitanya and Krishna [16] applied non-dominated sorting genetic algorithm-II (NSGA-II) for optimizing HAZ and SR in a pulsed Nd:YAG laser cutting process while considering four input variables, i.e., laser

power, pulse frequency, gas pressure and pulse width, and developed the Pareto optimal set of solutions. Mishra and Yadava [17] integrated finite element method and artificial neural network (ANN) to develop a prediction model for a laser beam percussion drilling (LBPD) process. The GRA along with principal component analysis was adopted for multi-objective optimization of the said LBPD process based on the data predicted by the ANN model. Madić et al. [18] performed multi-objective optimization of CO_2 laser cutting process considering three responses, i.e., SR, HAZ and kerf width based on four process parameters (laser power, cutting speed, assist gas pressure and focus position) while employing cuckoo search algorithm. Biswas et al. [19] optimized individually as well as simultaneously three hole qualities, i.e., hole diameter at entry, hole diameter at exit and hole taper in a pulsed Nd:YAG laser micro-drilling process. Ranjan and Mishra [20] determined the optimal parametric settings of a Nd:YAG laser beam machining process for performing micro-grooving operation on hydroxyapatite.

3. SHUFFLED FROG LEAPING ALGORITHM

Shuffled frog leaping algorithm (SFLA) principally incorporates two conventional optimization approaches, i.e., shuffled complex evolution (SCE) and PSO technique. The main philosophy behind SCE is the natural evolution. In this algorithm, at first, the population is divided into several sub-populations and allowed to interbreed independently. After a defined number of evolutions, all the sub-populations are forced to mix, and are again divided into several new sub-populations by means of shuffling. It helps in sharing information between different sub-populations, which they have independently developed over the course of evolution. On the other hand, PSO technique is motivated from the simulation of social patterns of different living things, e.g., a pattern based on the movement of ants, flocking pattern of birds etc. It involves memetic evolution of particles as swarm towards the best solution while improving the position of each particle based on the position of other particles with respect to the source of the optimal result.

3.1. A Brief Description of Shuffled Frog Leaping Algorithm

It is a memetic meta-heuristic algorithm designed to perform an informed heuristic search using a heuristic function so as to obtain solution of an optimization problem. As its name suggests, it is dependent on a population of memes (analogous to genes, except that information in genes can be transferred only from parent to an offspring, whereas,

information transfer in memes has a wider aspect, like transfer of an idea which can happen between any two individuals) to obtain an optimal result [21]. This algorithm is based on a virtual population of frogs and mimics the movement of frogs towards their search for the maximum food source. As it is derived from both SCE and PSO, first frogs leap from one position to another being influenced by the position of the frog which is in a better position from the food source and then shuffling of information among different groups of frogs occurs to approach towards the best solution, and hence, the name shuffled frog leaping algorithm is given to it [22].

The SFLA is based on a combination of both deterministic and random approaches. The deterministic strategy allows it to utilize response surface information to effectively guide the search process as in PSO algorithm, whereas, the random approach ensures flexibility and robustness of the heuristic search process. A randomly selected population of F frogs is generated over an entire pond. The population is partitioned into several complexes (subsequently referred to as memeplex), which are allowed to evolve independently in their own memeplex. All the frogs (memes) in a given memeplex share information within that group, i.e., the frogs are influenced by the ideas of other frogs. Thus, they undergo memetic evolution. It improves the quality of a meme and guides it towards a better performance (by evaluating the corresponding fitness). To ensure that the evolution is competitive, it is required that the better frogs contribute more to the evolution than the relatively poor frogs. So, a probabilistic approach is adopted for selecting memes for evolution inside a memeplex, where better frogs are given more weights, i.e., have a better chance of selection for evolution. During this evolution process, the target of the algorithm is to improve the quality of the worst frog with respect to the local best frog and subsequently, the global best frog. After evolution, there is a chance that the evolved frog may be of better quality or worse quality. If the evolved frog is of better quality, it is added back to the memeplex, else a new random frog is generated and added in place of the worse frog. The improved information after evolution is immediately available for subsequent iterations of the evolution. After a certain number of evolutions, the memeplexes are forced to mix together (i.e., global share of information) by a shuffling process and the population is again divided into several memeplexes. This global sharing of information (or in genetic term, cross-hybridization of frogs/ideas) expedites the searching process. It also ensures a proper cultural evolution without presence of any regional bias. One of the prime advantages of SFLA is its ability not to be get stuck in some local optima, rather move towards the global optima at a faster rate, owing to the memetic evolution within memeplexes as well as between memeplexes [23, 24].

3.2. Steps Involved in SFLA

The procedural steps of SFLA are presented in details here-in-under.

Global exploration

1. Initialize a virtual population of F frogs, and select m (number of memeplexes) and n (number of memes in each memeplex) such that $F = m \times n$.
2. Define d as the number of decision variables such that an i^{th} frog can be represented by a vector $U(i) = (U_1, U_2, U_3, \ldots, U_d)$ and calculate the performance value (i.e., fitness $f(i)$) of each frog $U(i)$.
3. Rank the frogs in decreasing order of their performance values such that the first rank represents the frog with the best fitness value. Record the position of the best frog as P_x.
4. Divide frogs into m memeplexes. This division must be based on the order of their ranks, serially, i.e., rank 1 in 1^{st} memeplex, rank 2 in 2^{nd} memeplex and so on, so that each memeplex has a fair share of the best and the worst frogs.
5. *Local exploration*
   i) Set $im = 0$ where im counts the number of memeplexes and will be compared with the total number m of memeplexes. Set $iN = 0$ where iN counts the number of evolutionary steps and will be compared with the maximum number N of steps to be completed within each memeplex.
   ii) Construct a sub-memeplex. As mentioned earlier, the aim of a frog is to leap towards an optimal solution, while improving their memes through evolution. The sub-memeplex selection criterion is to allocate more weights to the frogs with higher fitness values and less weight to the frogs with lower fitness values, using a probabilistic approach, where p_j denotes the probability of selection of j^{th} frog to the sub-memeplex.

$$p_j = \frac{2(n+1-j)}{n(n+1)} \quad \text{for all } j = 1,2,\ldots,n \tag{1}$$

   It ensures that the frog with higher fitness value has a greater chance to be selected in the sub-memeplex. Here, q distinct frogs are selected randomly from each memeplex. Record the position of the best frog and the worst frog in the sub-memeplex as P_b and P_w.
   iii) Improve the position of the worst frog using the following equation,step size $S = \min\{\text{int}[\text{rand}(P_b - P_w)], S_{max}\}$ for a positive step andstep size $S = \max\{\text{int}[\text{rand}(P_b - P_w)], -S_{max}\}$ for a negative step, where rand is a random number between 0 and 1, and S_{max} is the maximum step allowed for leaping of an infected frog. The new position is then computed by $U(q) = P_w + S$. If

the new position is within the feasible search region, then calculate the new fitness value $f(q)$. Otherwise, go to step (iv). If the new $f(q)$ is better than the previous fitness value of the frog, then replace the old $U(q)$ with the new $U(q)$, and proceed to step (vi). Otherwise, go to step (iv).

iv) If step (iii) cannot produce a better result, then the step and the new position are again calculated with respect to the global best frog, as follows, step size $S = \min\{\text{int}[\text{rand}(P_x - P_w)], S_{max}\}$ for a positive step and step size $S = \max\{\text{int}[\text{rand}(P_x - P_w)], -S_{max}\}$ for a negative step, and the new position is computed as $U(q) = P_w + S$. If the new $U(q)$ is within the feasible search space, compute its fitness value or else go to step (v). If the new $f(q)$ is better than the previous value, then replace the old $U(q)$ with the new $U(q)$ and go to step (vi). Otherwise, go to step (v).

v) If the new position obtained is either infeasible or is not better than the old position, a new randomly generated frog r replaces the worst frog with $U(q) = r$ and $f(q) = f(r)$.

vi) Upgrade the memeplex and proceed evolution for a definite number of iterations. Repeat steps (i)-(v) for all m memeplexes.

6. Shuffle the memeplexes. Sort the population again in order of decreasing fitness values and repeat steps (1)-(5).
7. Stop the iteration after a definite number of runs.

The pseudo code of SFLA is provided as below:

Begin;
Generate random population of F solutions (frogs);
For each individual $i \in F$, calculate fitness(i);
Sort the population F in descending order of their fitness;
Divide F into m memeplexes;
For each memeplex, determine the best and the worst frogs;
Improve the worst frog position using appropriate equations;
Repeat for a specific number of iterations;
End;
Combine the evolved memeplexes;
Sort the population F in descending order of their fitness;
Check if termination = true;
End;

3.3. Optimization Parameters in SFLA

It is evident from the framework of SFLA model that there are several significant parameters on which its final solution depends. Thus, selection of the best possible parameters for achieving the most satisfactory optimization results becomes quite critical. It can be noticed that SFLA has five parameters, i.e., number m of memeplexes, number n of frogs in a memeplex, number q of frogs in a sub-memeplex, number N of evolutions in a memeplex between two successive shufflings, and maximum step size S_{max} allowed during an evolutionary step.

Theoretically, the sample size F (i.e., number of memeplexes multiplied by the number of frogs in each memeplex) is supposed to be the most influential parameter. The chance of reaching a global optimal value increases with increasing population size. However, a correct balance must be maintained between the values of m and n. A large value of m and a small value of n mean very less amount of local change of information, and the purpose of SFLA is to build up a strategy to take into consideration both the global and local search processes. So, while selecting the value for m, the value of n must not be selected too less than m. The response of the algorithm with respect to parameter q, i.e., number of frogs in a sub-memeplex, is that the local evolution will be slow for higher values of q, resulting in longer times to reach the optimal solution. The other parameter, N, can take any value larger than 1. If N is small, the memeplexes will shuffle frequently, reducing the information exchange at local level. If N is too large, there will be too much of idea changes at local level so that each memeplex will turn into a local optimal. The last parameter is the maximum step size S_{max}. It is the maximum leaping ability of a frog after it is being infected by an idea. It decides the amount of global exploration ability of a frog. Setting it to a smaller value reduces the sole purpose of global exploration, however setting it to a larger value, may result in missing the actual optima. Hence, a fine balance is to be sought out for selection of S_{max} value. Although all these are theoretical, there is no proper guidance for selection of these parameter values. In this chapter, an experimental approach is provided to investigate the influence of these parameters on the optimization performance of SFLA. Figures 1-3 exhibit a pictorial representation of SFLA. On the other hand, Figure 4 demonstrates the flowchart of SFLA and Figure 5 represents the local search flowchart of this algorithm.

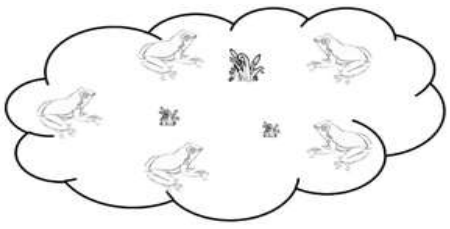

Figure 1. Population of frogs divided into memeplexes.

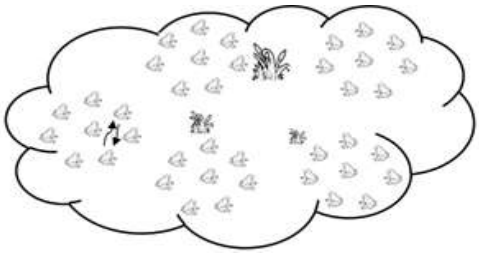

Figure 2. Local evolution: Idea sharing within memeplex.

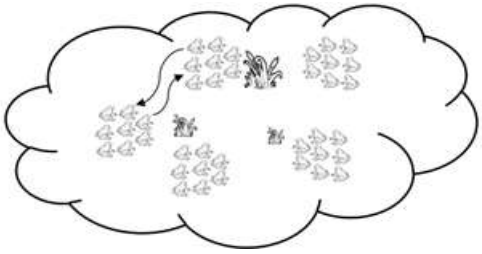

Figure 3. Global exploration: Shuffling of memeplexes.

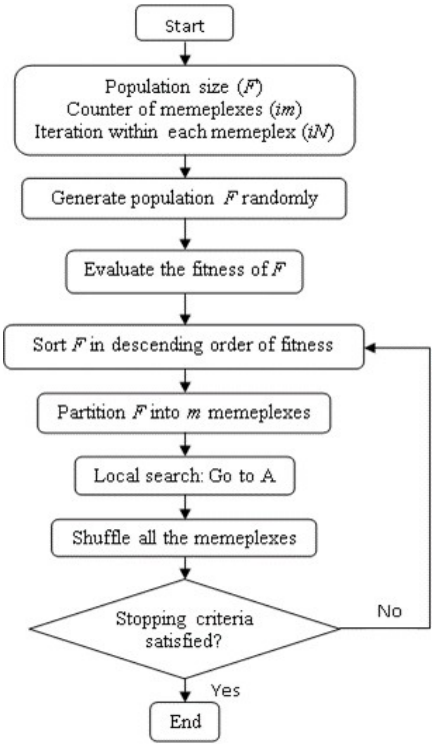

Figure 4. SFLA flowchart.

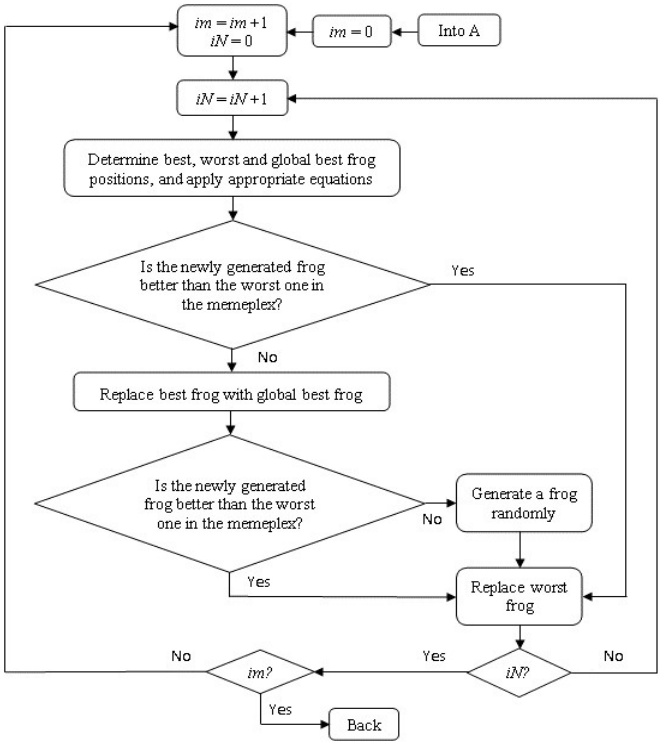

Figure 5. Local search flowchart of SFLA.

4. LASER BEAM MACHINING PROCESS OPTIMIZATION USING SFLA

Based on the pseudo code of SFLA as stated above, the corresponding MATLAB code is subsequently developed in order to validate the effectiveness and potentiality of SFLA for parametric optimization of two LBM processes.

4.1. Example 1

Kuar et al. [25] performed laser beam micro-drilling operation on zirconia (ZrO_2) ceramics of size 20×20 mm and 1 mm thickness, and investigated the influences of four process parameters, i.e., lamp current, pulse frequency, air pressure and pulse width on HAZ thickness and taper of the drilled holes. Each of those four process parameters was set at five different levels, as shown in Table 1. In order to determine the multi-parametric optimal combinations for pulsed Nd:YAG laser beam micro-drilling process on ZrO_2 ceramics, experiments were conducted according to a central composite rotatable second-order design plan based on RSM technique, and the following two equations were developed for HAZ thickness and taper.

Table 1. Process parameters and their settings for example 1

Parameter	Unit	Symbol	Levels				
			-2	-1	0	1	2
Lamp current	A	x_1	17	19	21	23	25
Pulse frequency	kHz	x_2	1	2	3	4	5
Air pressure	kg/cm^2	x_3	0.6	1	1.4	1.8	2.2
Pulse width	%	x_4	2	6	10	14	18

$$Y_{HAZ} = 0.3796 + 0.07888x_1 - 0.04120x_2 - 0.04301x_3 - 0.00570x_4 + 0.02146x_1^2 - 0.00957x_2^2 + 0.00266x_3^2 - 0.01234x_4^2 - 0.0228x_1x_2 - 0.00679x_1x_3 - 0.03158x_1x_4 + 0.01341x_2x_3 - 0.00983x_2x_4 - 0.00497x_3x_4 \quad (2)$$

$$Y_{TAPER} = 0.07253 + 0.00912x_1 + 0.00887x_2 - 0.00606x_3 + 0.00449x_4 + 0.00153x_1^2 + 0.00225x_2^2 + 0.00233x_3^2 + 0.00399x_4^2 + 0.00431x_1x_2 - 0.00646x_1x_3 - 0.00519x_1x_4 - 0.00110x_2x_3 - 0.00023x_2x_4 - 0.07253x_3x_4 \quad (3)$$

These two second-order RSM-based equations are separately optimized applying SFLA within the respective ranges of values for the considered process parameters. The results of single objective optimization are provided in Table 2.

Table 2. Results of single objective optimization for example 1

Optimization method	Response	Optimal value	x_1	x_2	x_3	x_4
Desirability function [25]	HAZ	0.0675	17	2	2	2
	Taper	0.0319	17	2	0.6	2
GA	HAZ	0.1066	19	1	2	2
	Taper	0.0843	23.86	2.29	1.38	13.92
PSO	HAZ	0.0604	18	1.25	2.12	2.4
	Taper	0.0458	20.23	4.10	1.81	11.95
ACO	HAZ	0.0324	17	1.5	2	2
	Taper	0.0377	18.04	4.47	1.73	14.18
ABC	HAZ	0.0174	17	4.8	2.1	2
	Taper	0.0202	18.2	1.25	0.6	2
SFLA	HAZ	0.0000010	17.23053	1.00266	2.19366	2.49103
	Taper	0.0000012	17.24257	1.02715	2.14176	2.22312

The single objective optimization results of Table 2 depict that SFLA performs fairly well in comparison to other algorithms, such as GA, PSO, ant colony optimization (ACO) and ABC [14]. It thus clearly outperforms the other population-based algorithms while

achieving the best possible solutions. The mean and standard deviation values of the optimal solutions as derived employing the considered algorithms are also provided in Table 3. Low standard deviation for SFLA indicates that the derived optimal solutions are highly repetitive in nature and close to the target values.

Multi-objective optimization of the responses for the considered LBM process is also attempted using SFLA and the achieved results are compared with those obtained from the other algorithms. For multi-objective optimization of the responses, the following objective function is developed:

$$z = \frac{w_1 \times Y_{HAZ}}{\text{HAZ}_{\min}} + \frac{w_2 \times Y_{TAPER}}{\text{Taper}_{\min}} \tag{4}$$

where w_1 and w_2 are the respective weights allotted to two different responses, i.e., HAZ and taper. The multi-objective optimization results for this example are tabulated in Table 4.

Table 3. Mean and standard deviation values for single objective optimization results

Optimization method	Response	Optimal value	Mean	Standard deviation
GA	HAZ	0.1066	0.1231	0.0102
	Taper	0.0843	0.1056	0.0151
PSO	HAZ	0.0604	0.0883	0.0212
	Taper	0.0458	0.0662	0.0138
ACO	HAZ	0.0324	0.0505	0.0129
	Taper	0.0377	0.0507	0.0098
ABC	HAZ	0.0174	0.0301	0.0094
	Taper	0.0202	0.0346	0.0092
SFLA	HAZ	0.0000010	0.00000458	0.000005
	Taper	0.0000012	0.00003030	0.000044

Table 4 exhibits the multi-objective optimization results for three cases considering different weight combinations for HAZ and taper. These results indicate a significant improvement in the optimal solutions of multi-objective optimization using SFLA as compared to other algorithms, like ABC algorithm [14]. The relevant scatter plots of Figures 6-7 are developed in order to study the variations of the responses with respect to four LBM process parameters. These plots show the quick convergence of SFLA towards the optimal solutions. As opposed to response surface plots, scatter plots are not portrayed by holding any parametric value constant and thus indicate the true trend of the output responses with respect to different process parameters.

Table 4. Multi-objective optimization results for example 1

Case	Response	Optimal value	x_1	x_2	x_3	x_4
Desirability function [25]	HAZ	0.1296	17	1.62	1.04	2
	Taper	0.0400				
ABC algorithm						
Case 1: $w_1 = 0.5$ and $w_2 = 0.5$	HAZ	0.1019	17.18	1.5	1.33	2
	Taper	0.0248				
Case 2: $w_1 = 0.9$ and $w_2 = 0.1$	HAZ	0.0281	17.2	1.5	2.16	2
	Taper	0.3733				
Case 3: $w_1 = 0.1$ and $w_2 = 0.9$	HAZ	0.3124	18.66	1.34	1.20	7.95
	Taper	0.0329				
SFLA						
Case 1: $w_1 = 0.5$ and $w_2 = 0.5$	HAZ	0.07352	17	1	1.26	2
	Taper	0.00057				
Case 2: $w_1 = 0.9$and $w_2 = 0.1$	HAZ	0.00434	17.2056	1.0405	2.0254	2.0122
	Taper	0.29960				
Case 3: $w_1 = 0.1$ and $w_2 = 0.9$	HAZ	0.29809	19.4696	4.1153	1.0529	6.8233
	Taper	0.02526				

From Figure 6, it is evident that HAZ thickness tends towards optimality with decrease in pulse frequency, pulse width and lamp current. However, with increase in assist air pressure, HAZ tends towards its minimum value. Similarly, from Figure 7, it can be observed that taper moves towards its optimal value with decrease in pulse frequency and increase in lamp current. Air pressure and pulse width show almost similar patterns towards achieving the optimal taper value, i.e., minimal taper can be obtained while maintaining air pressure and pulse width nearer to their central values in the combinational settings. Similar types of observations were also investigated by Kuar et al. [25].

In this chapter, a maiden attempt is also taken to provide some valuable guidance on how to identify the correct algorithmic parameter settings while using SFLA as an effective optimization tool. Thus, the variations in the optimal solutions are studied while changing the settings of different algorithmic parameters in SFLA. The top two performances for each parametric setting from a set of simulation runs are summarized through Tables 5-8.

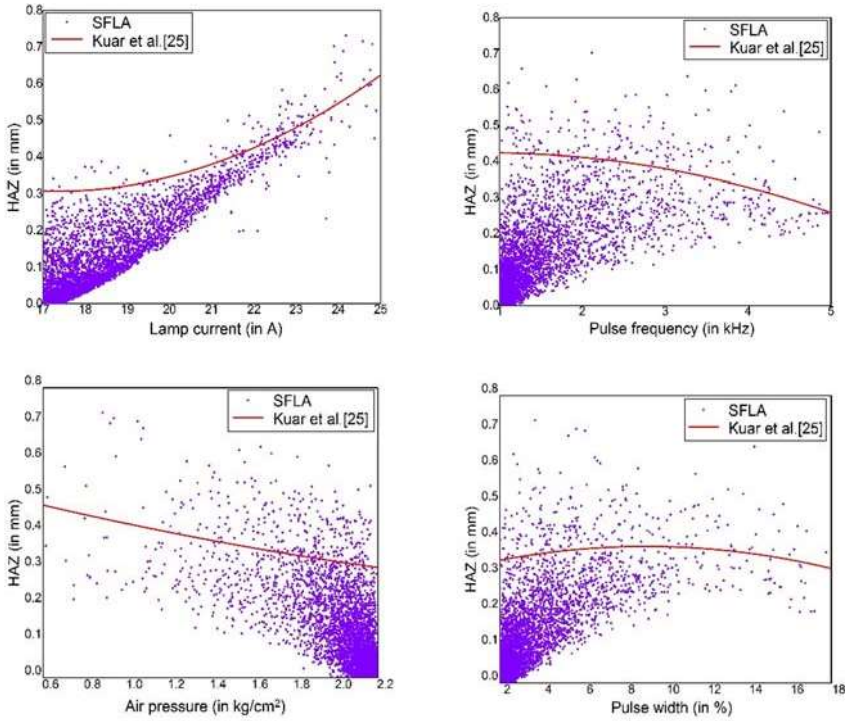

Figure 6. Variation of HAZ with respect to different process parameters.

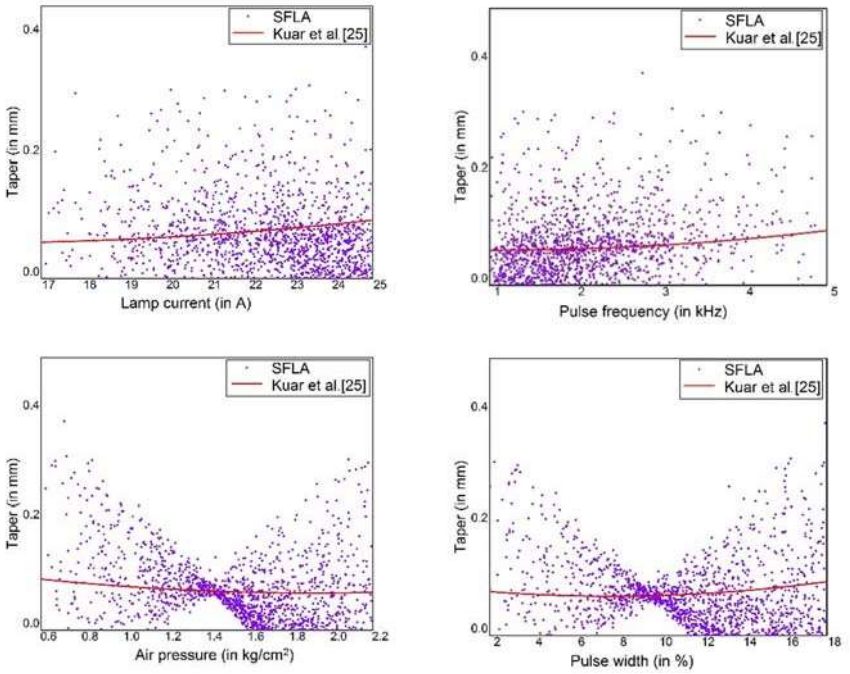

Figure 7. Variation of taper with respect to different process parameters.

Table 5. Variation in optimal solution with respect to sample size

x_1	x_2	x_3	x_4	Response (HAZ)
Population size = 100				
17.5235	1.0015	2.1982	2.0036	0.0000192
17.5081	1.0004	2.1930	2.0177	0.0000183
Population size = 200				
17.2839	1.0545	2.1961	2.2527	0.0000180
17.3543	1.0056	2.1533	2.1382	0.0000076
Population size = 500				
17.2896	1.0678	2.1553	2.0693	0.0000021
17.0566	1.1320	2.1383	2.1953	0.0000019

Table 6. Variation in optimal solution with respect to maximum step size

x_1	x_2	x_3	x_4	Response (HAZ)
Maximum step size = 2				
17.3145	1.0631	2.1664	2.0771	0.0000015
17.2305	1.0026	2.1936	2.4910	0.0000010
Maximum step size = 3				
17.4893	1.0101	2.1960	2.0314	0.0000040
17.3227	1.0249	2.1612	2.1608	0.0000013
Maximum step size = 5				
17.3335	1.0435	2.1671	2.1061	0.0000051
17.1332	1.1374	2.1818	2.1970	0.0000066

Table 7. Variation in optimal solution with respect to sub-memeplex size

x_1	x_2	x_3	x_4	Response (HAZ)
Sub-memeplex size = 3				
17.2667	1.1084	2.1898	2.3703	0.0000019
17.5176	1.0007	2.1945	2.0037	0.0000035
Sub-memeplex size = 4				
17.5077	1.0109	2.1998	2.0088	0.0000024
17.4907	1.0067	2.1971	2.0435	0.0000018
Sub-memeplex size = 5				
17.3335	1.0435	2.1671	2.1061	0.0000051
17.3360	1.0371	2.1768	2.1536	0.0000016

Tables 5-8 depict that selection of the most appropriate algorithmic parameters for SFLA plays an important role in achieving the optimal solutions. The more is the population size, the better are the results. For maximum step size, the lesser is the step size, the more accurate is the solution. Increasing step size may lead to loss of the actual optimal solutions. The sub-memeplex size, as stated earlier, should not be too small or too large and thus, choosing a proper sub-memeplex size is also critical for better performance of this algorithm. Lastly, the number of evolutions in a memeplex between successive shufflings must not be too small because it will destroy the whole notion of local exchange of ideas. However, selection of too large a value may often lead to slower convergence of the solutions.

Table 8. Variation optimal solution with respect to number of local evolutions

x_1	x_2	x_3	x_4	Response (HAZ)
Number of local evolutions = 2				
17.0407	1.0462	2.1063	2.3710	0.0000313
17.2543	1.0266	2.1772	2.3240	0.0000183
Number of local evolutions = 3				
17.2617	1.0226	2.1792	2.3300	0.0000070
17.3212	1.0490	2.1495	2.0524	0.0000112
Number of local evolutions = 5				
17.4828	1.0138	2.1914	2.0161	0.0000025
17.4147	1.0308	2.1897	2.0801	0.0000018

4.2. Example 2

Dhupal et al. [26] performed laser turning operation for micro-groove generation on cylindrical ceramic materials using a CNC-controlled pulse Nd:YAG laser machining system. A cylindrical aluminium oxide workpiece of size of 10 mm diameter and 40 mm length was taken, and the laser beam was focused using a lens having a focal length of 50 mm. The focal plane of the laser beam was set at the surface of the rotating cylindrical workpiece. The laser beam spot size was approximately 0.1 mm. The specimen was micro-grooved using multiple laser pulses with actual peak powers ranging between 0.7 and 5 kW. It was held by a collet attached to a stepper motor which would help to rotate the collet and job simultaneously. A micro-controller was utilized along with a stepper motor to achieve the desired rotation in anti-clockwise or clockwise direction. The Z-axis movement was given to the lens through a program after each pass in order to obtain the required depth. The whole system was monitored using a computer vision system.

A combined methodology based on RSM-ANN-GA approach was adopted for multi-parametric study of the laser turning process for micro-grooving operation on the selected specimen. Design of experiments was utilized for conducting the laser-turned micro-grooving operation, and the responses from different parametric combinations were employed for ANN development and subsequent deployment of GA for the optimized minimum deviations. The selected process parameters along with their ranges of values are specified in Table 9. Using experimental results, three RSM-based equations were developed for deviation in upper width (Y_{uw}), deviation in lower width (Y_{lw}) and deviation in depth (Y_d). The target output was set at 0.2 mm and the deviations were recorded accordingly.

Table 9. Process parameters and their settings for example 2

Parameter	Unit	Symbol	Levels				
			-2	-1	0	1	2
Air pressure	N/mm^2	x_1	0.03	0.08	0.13	0.18	0.23
Lamp current	A	x_2	13	16	19	22	25
Pulse frequency	kHz	x_3	1	2	3	4	5
Pulse width	%	x_4	2	4	6	8	10
Cutting speed	rpm	x_5	7	12	17	22	27

$$Y_{uw} = -0.00376 - 0.0169x_1 - 0.00251x_2 - 0.00288x_3 + 0.00048x_4 + 0.00185x_5 + 0.00678x_1^2 + 0.00232x_2^2 + 0.00276x_3^2 - 0.00012x_4^2 + 0.00207x_5^2 + 0.00004x_1x_2 - 0.00134x_1x_3 + 0.00188x_1x_4 - 0.00225x_1x_5 - 0.00149x_2x_3 - 0.00081x_2x_4 - 0.00052x_2x_5 + 0.00114x_3x_4 - 0.00262x_3x_5 + 0.0012x_4x_5 \quad (5)$$

$$Y_{lw} = 0.01857 - 0.0133x_1 - 0.00247x_2 - 0.00268x_3 + 0.0012x_4 - 0.00391x_5 + 0.00299x_1^2 + 0.00224x_2^2 - 0.00137x_3^2 - 0.00122x_4^2 + 0.00051x_5^2 + 0.00235x_1x_2 - 0.00122x_1x_3 - 0.00168x_1x_4 + 0.00197x_1x_5 - 0.00197x_2x_3 - 0.00175x_2x_4 + 0.00166x_2x_5 - 0.0078x_3x_4 - 0.00211x_3x_5 + 0.00378x_4x_5 \quad (6)$$

$$Y_d = 0.01265 - 0.0251x_1 - 0.00263x_2 + 0.00451x_3 + 0.00479x_4 - 0.00229x_5 + 0.00338x_1^2 + 0.0038x_2^2 - 0.00168x_3^2 + 0.00157x_4^2 - 0.00112x_5^2 - 0.00214x_1x_2 - 0.00472x_1x_3 - 0.00264x_1x_4 + 0.0026x_1x_5 - 0.00035x_2x_3 - 0.00314x_2x_4 - 0.00365x_2x_5 - 0.00425x_3x_4 + 0.00006x_3x_5 + 0.00393x_4x_5 \quad (7)$$

Dhupal et al. [26] applied the traditional GA technique to optimize those responses and for multi-objective optimization, obtained values of −0.0101, 0.0098 and −0.0069

mm respectively for upper width, lower width and depth deviations with the parametric settings as lamp current = 19 A, pulse frequency =3.2 kHz, pulse width = 6% of duty cycle, air pressure = 0.13 N/mm^2 and cutting speed = 22 rpm. The multi-objective optimization results using SFLA are provided in Table 10 and compared with those derived while applying the traditional GA technique. For multi-objective optimization, the objective function is set as minimization of $z=|Y_{uw}|+|Y_{lw}|+|Y_d|$, since the aim of this optimization problem is to simultaneously minimize all the considered deviations in upper width, lower width and depth.

Table 10. Multi-objective optimization results for example 2

Technique	Process parameters					Responses		
	x_1	x_2	x_3	x_4	x_5	Y_{uw}	Y_{lw}	Y_d
GA	19	3.2	6	0.13	22	-0.01010	0.00980	-0.00690
SFLA	14.5	2.3	4.72	0.805	23.75	0.00017	-0.00004	0.00041

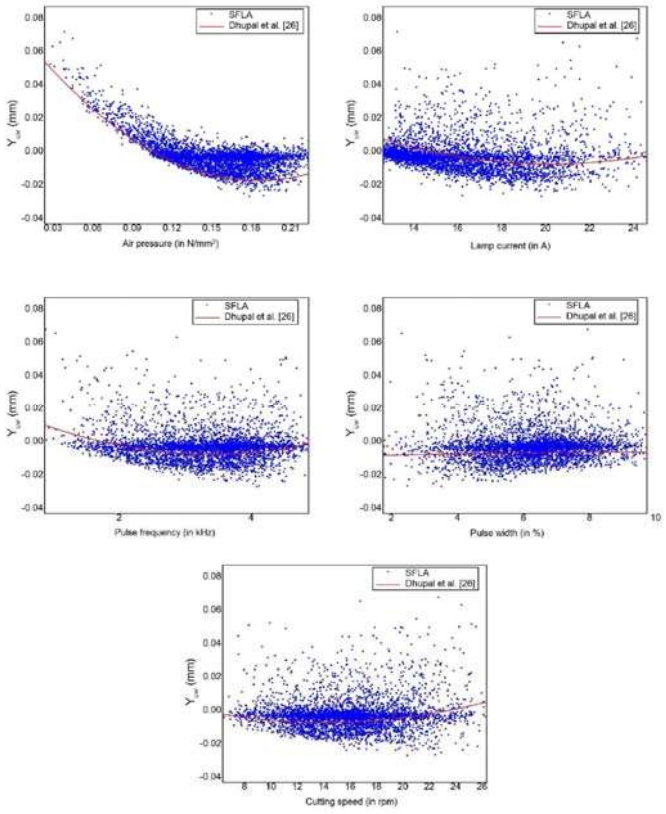

Figure 8. Variation in upper width deviation with respect to different process parameters.

From Table 10, it becomes quite evident that SFLA excels over the traditional GA technique while providing better optimal solutions. The scatter plots developed showing the changes of the considered deviations with respect to varying values of five process parameters are depicted in Figures 8-10. Since no parameter is held constant here, unlike in response surfaces, scatter plots better provide the overall trend of the responses for different process parameters. Since all the considered deviations need to be minimized, it is apparent from these scatter plots that maximum cluster of points are concentrated near the zero deviation, demonstrating high convergence rate of SFLA.

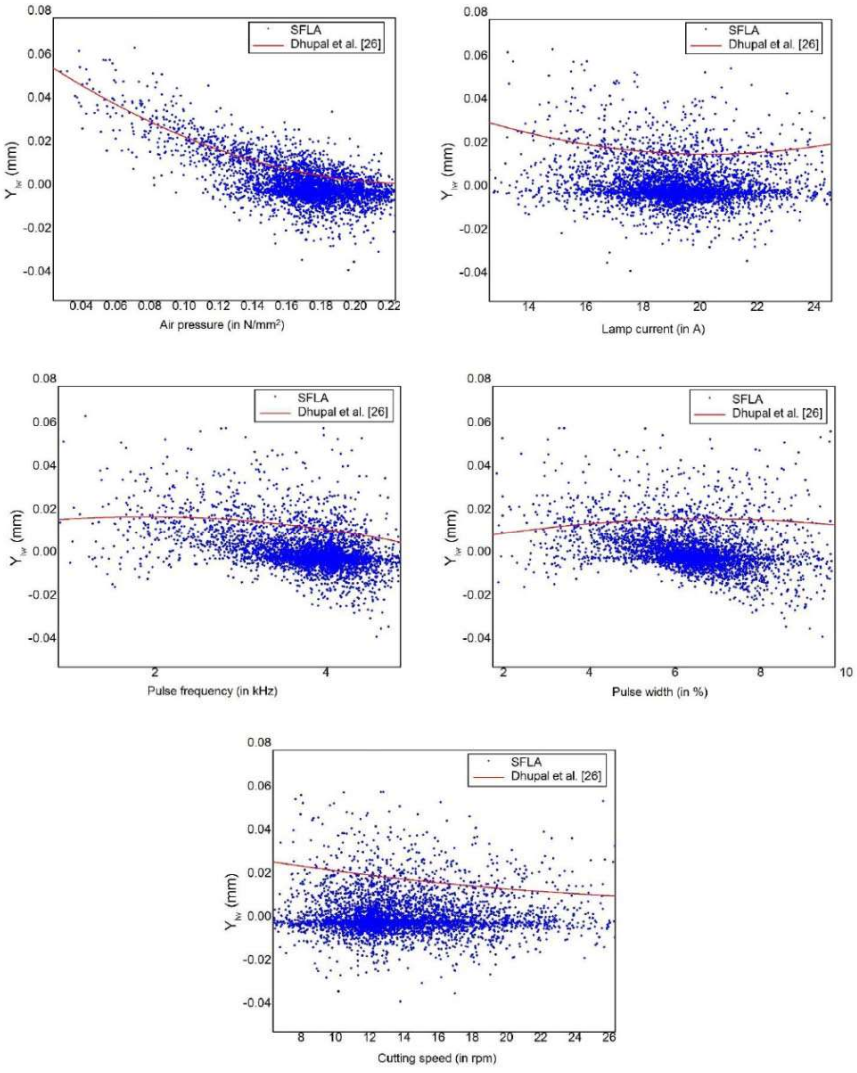

Figure 9. Variation in lower width deviation with respect to different process parameters.

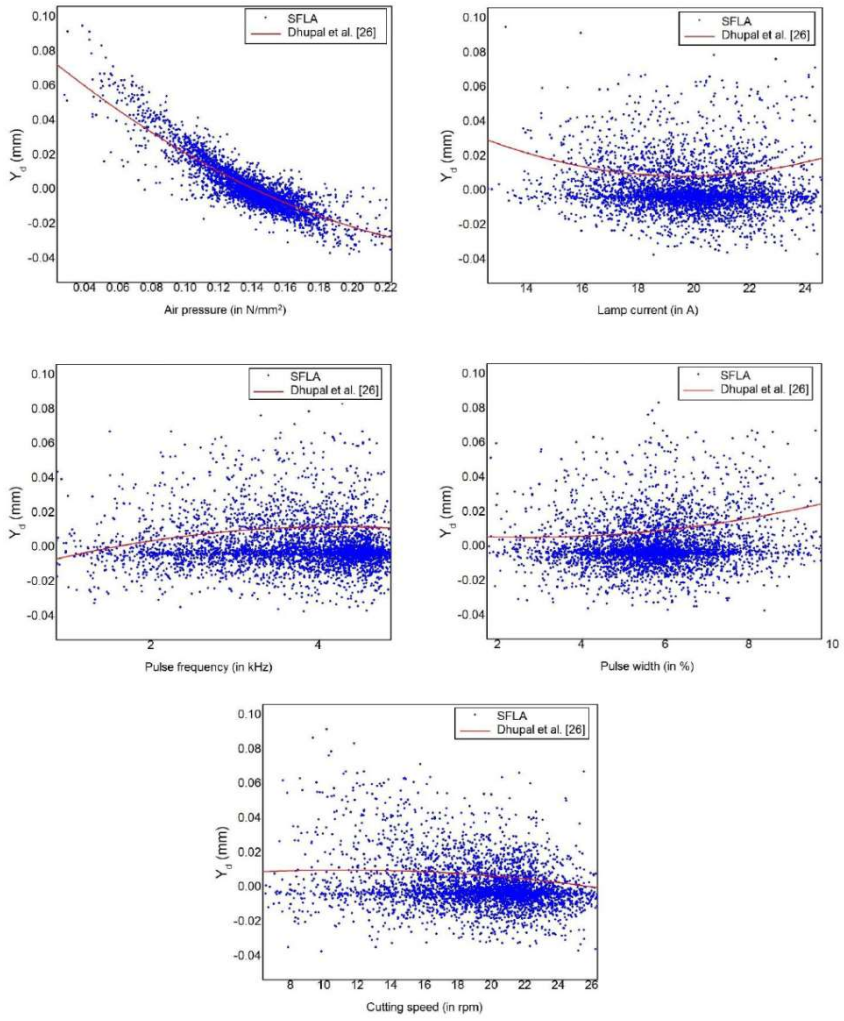

Figure 10. Variation in depth deviation with respect to different process parameters.

CONCLUSION

In this chapter, parametric optimization of two laser beam machining processes are carried out employing an almost novel meta-heuristic approach in the form of shuffled frog leaping algorithm. The results derived for single as well as and multi-objective optimization using SFLA are observed to be better when compared to other algorithms, like GA, ABC, ACO, PSO etc. The calculated mean and standard deviation values are utilized so as differentiate between the performance of different algorithms with respect to the repeatability of the algorithm towards attaining the optimal solutions in successive runs. It is evident that SFLA is successful in providing consistent results in successive runs. In order to investigate the effects of various algorithmic parameters of SFLA on

solution accuracy, experiments are also conducted which show that the sample size in this algorithm plays a significant role in obtaining better results. The values for maximum step size, sub-memeplex size and number of intra-memeplex evolutions are also supposed to be influential for the success of SFLA. The successful application of this algorithm in optimizing responses of other non-traditional machining processes, like wire electrical discharge machining, plasma arc machining, water and abrasive water jet machining etc. may be the direction of future research works.

REFERENCES

[1] Dubey, A.K., Yadava, V., (2008). Laser beam machining: A review. *Int. J. Mach. Tool. Manu.* 48, 609-628.

[2] Majumdar, J.D., Manna, I., (2003). Laser processing of materials. *Sadhana* 28, 495-562.

[3] Norikazu, T., Shigenori, Y., Masao, H., (1996). Present and future of lasers for fine cutting of metal plate. *J. Mater. Process. Tech.* 62, 309-314.

[4] Meijer, J., (2004). Laser beam machining (LBM), state of the art and new opportunities. *J. Mater. Process. Tech.* 149, 2-17.

[5] Voisey, K.T., Cheng, C.F., Clyne, T.W., (2000). Quantification of melt ejection phenomena during laser drilling. *Mater. Res. Soc.* 617, J5.6.1-J5.6.7.

[6] Lau, W.S., Lee, W.B., (1992). Pulsed Nd:YAG laser cutting of carbon fibre composite materials. *Ann. CIRP* 39, 179-182.

[7] Rao, B.T., Kumar, H., Nath, A.K., (2005). Processing of concretes with a high-power CO_2 laser. *Opt. Laser Technol.* 37, 348-356.

[8] Chen, S.L., (1999). The effects of high-pressure assistant-gas flow on high-power CO_2 laser cutting. *J. Mater. Process. Tech.* 88, 57-66.

[9] Rajaram, N., Ahmad, J.S., Cheraghi, S.H., (2003). CO_2 laser cut quality of 4130 steel. *Int. J. Mach. Tool. Manu.* 43, 351-358.

[10] Ganguly, D., Acherjee, B., Kuar, A.S., Mitra, S. (2012). Hole characteristics optimization in Nd:YAG laser micro-drilling of zirconium oxide by grey relation analysis. *Int. J. Adv. Manuf. Tech.* 61, 1255-1262.

[11] Pandey, A.K., Dubey, A.K., (2012). Simultaneous optimization of multiple quality characteristics in laser cutting of titanium alloy sheet. *Opt. Laser Technol.* 44, 1858-1865.

[12] Pandey, A.K., Dubey, A.K., (2012) Taguchi based fuzzy logic optimization of multiple quality characteristics in laser cutting of Duralumin sheet. *Opt. Laser. Eng.* 50, 328-335.

[13] Teixidor, D., Ferrer, I., Ciurana, J., Özel, T., (2013). Optimization of process parameters for pulsed laser milling of micro-channels on AISI H13 tool steel. *Robot. Cim-Int. Manuf.* 29, 209-218.

[14] Mukherjee, R., Goswami, D., Chakraborty, S., (2013). Parametric optimization of Nd:YAG laser beam machining process using artificial bee colony algorithm. *J. Ind. Eng.* 15 pages, http://dx.doi.org/10.1155/2013/570250.

[15] Pandey, A.K., Dubey, A.K., (2013). Multiple quality optimization in laser cutting of difficult-to-laser-cut material using grey-fuzzy methodology. *Int. J. Adv. Manuf. Tech.* 65, 421-431.

[16] Chaitanya, L., Krishna, G., (2013). Multi-objective optimization of laser beam cutting process. *Int. J. Res. Mech. Eng. Technol.* 3, 279-290.

[17] Mishra, S., Yadava, V., (2013). Modeling and optimization of laser beam percussion drilling of nickel-based superalloy sheet using Nd:YAG laser. *Opt. Laser. Eng.* 51, 681-695.

[18] Madić, M., M. Radovanović, Trajanović, M., ManiIć, M., (2015). Multi-objective optimization of laser cutting using cuckoo search algorithm. *J. Eng. Sci. Technol.* 10, 353-363.

[19] Biswas, R., Kuar, A.S., Mitra, S., (2015). Process optimization in Nd:YAG laser microdrilling of alumina-aluminium interpenetrating phase composite. *J. Mater. Res. Technol.* 4, 323-332.

[20] Ranjan, R., Mishra, A., (2016). Parametric optimization of laser beam micro-grooving of hydroxyapatite.*Arab. J.Sci.Eng.* 41, 4607-4612.

[21] Eusuff, M., Lansey, K., Pasha, F., (2006). Shuffled frog leaping algorithm: A memetic meta-heuristic for discrete optimization. *Eng. Optimiz.* 38, 129-154.

[22] Eusuff, M.M., Lansey, K.E. (2003). Optimization of water distribution network design using the shuffled frog leaping algorithm. *J. Water Res. Plan. Manage.* 129, 10-25.

[23] Luo, X-H., Yang,Y.,Li, X., (2008). Solving TSP with shuffled frog-leaping algorithm. *Proc. 8th Int.Con.*Intel. Sys. Des. App. 228-232.

[24] Rahimi-Vahed, A., Mirzaei, A.H., (2008). Solving a bi-criteria permutation flow-shop problem using shuffled frog-leaping algorithm. *Soft Comput.* 12, 435-452.

[25] Kuar, A.S., Doloi, B., Bhattacharyya, B., (2006). Modelling and analysis of pulsed Nd:YAG laser machining characteristics during micro-drilling of zirconia (ZrO_2). *Int. J. Mach. Tool. Manu.* 46, 1301-1310.

[26] Dhupal, D., Doloi, B., Bhattacharyya, B., (2008). Pulsed Nd:YAG laser turning of micro-groove on aluminum oxide ceramic (Al_2O_3). *Int. J. Mach. Tool. Manu.* 48, 236-248.